Light & Engineering
Vol. 29, No. 6, pp. 34–42, 2021

https://doi.org/10.33383/2020-059
Svetotekhnika # 4, pp. 5–11

THE EXPERIMENTAL RESEARCH INSTALLATION FOR THE DETERMINATION OF MONOCHROMATIC THRESHOLDS OF HUMAN VISUAL SYSTEM

George V. Boos, Andrey A. Grigoryev*,
and Victoria A. Rybina

National Research University Moscow Power Engineering Institute (NRU MPEI), Moscow
**E-mail: aag.2010@yandex.ru*

ABSTRACT

Relying on the statistical theory of the human threshold colour vision, the authors have developed the method how to determine the colour-matching functions of the physiological colorimetric system $(KZS)_{phys}$[1]. To implement the developed method, the authors have created the experimental research installation that allows them to determine the threshold characteristics of the visual system during the observation of monochromatic objects against coloured backgrounds. The authors have studied the inaccuracies of the experimental installation and of the algorithm for solving a system of nonlinear equations that allows them to determine the colour-matching functions of the physiological colorimetric system according to the results of the experiment.

Keywords: color-matching functions *(CMF)*, dichromats, trichromats, statistic theory, threshold characteristics of vision, object detection, experimental research installation

1. INTRODUCTION AND FORMULATION OF A PROBLEM

The spectral sensitivities of the long-wavelength-sensitive (L-), middle-wavelength-sensitive (M-) and short-wavelength-sensitive (S-) wavelength-sensitive cone types may be used both for conventional calculations of tristimulus values in the physiological colorimetric system and for consideration of colour adaptation when calculating colour rendering index of a light source. Therefore, any inaccuracy in their definition leads to errors in colour calculations. The conventional method of determination of these sensitivities is based on experiments on radiation chromaticity matching by dichromats. The methodology of such studies and the results of experiments with use of dichromats were published by Nyberg and Yustova in 1948 [1]. In 2006, the *TC 1–36* technical committee of CIE published the report [2] (*CIE2006 Physological Observer*, hereinafter referred to as *CIEPO06*) on selection of a set of *colour-matching functions* (*CMF*) and evaluations of *cone fundamentals* (by which the authors mean spectral responsivity functions of eye receptors measured in a cornea plane) for an observer with normal colour vision.

The *CIEPO06* model is primarily based on the works by A. Stockman and B. Sharpe [3, 4]. The experimental studies in [5] were conducted using the method, leading to isolation of one type of cones and involving dichromats as spectator instead of trichromats.

[1] In Russia, there is a concept of a physiological colorimetric system in which the colour-matching functions coincide with the spectral sensitivities of the L-cones, M-cones and S-cones. The colorimetric notation $(KZS)_{phys}$ is composed of capital letters of receptor types in Russian (krasnyy, zelenyy, siniy).

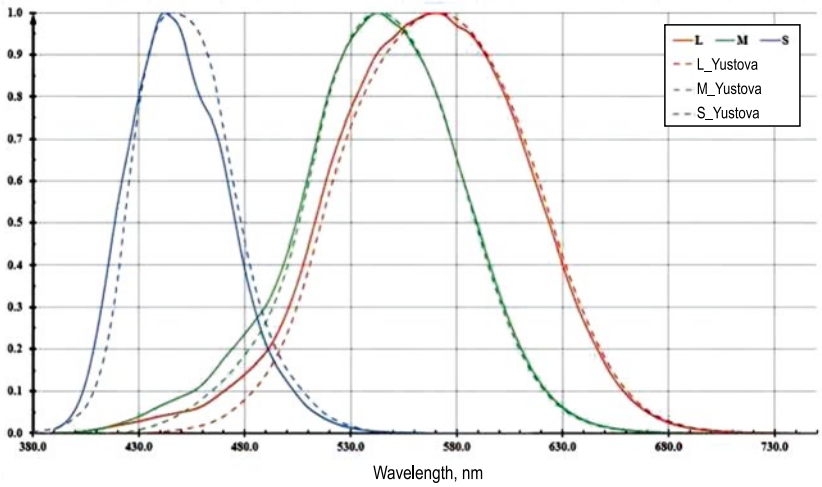

Fig. 1. The colour-matching functions of the physiological colorimetric system according to E.N. Yustova [1] and the spectral sensitivities of the L-cones, M-cones and S-cones A. Stockman [6] when **dichromates** is used as observers (relative units)

In 2019, Stockman [6] published the *CMF*-to-*XYZ* transfer matrix. Fig. 1 shows the colour-matching systems per unit in accordance with *CIEPO06* obtained using dichromats selected based on a DNA test and as per Yustova who used ordinary dichromats. It is seen that the curves obtained using different methods with different sets of spectators correspond well with each other, which indicates that the results are reliable, but it is relevant only in the case of dichromats.

There are still doubts about the legitimacy of the approach using dichromate instead of trichromatic since the human vision system (VS) colour-matching functions are defined not only by spectral sensitivity of cones, which may be identified using DNA tests. Human luminance and chromaticity perceptions appear not at receptor outputs but after their signals are processed by the brain using an algorithm (yet unknown) which may be completely different in the cases of trichromats who process signals from three receptors and dichromats who do not have one of the receptors but still perceive colours. To confirm or to waive the said doubts, it was necessary:

– To develop the methodology of **trichromat's** colour-matching functions of the physiological colorimetric system $(KZS)_{phys}$ calculation in conditions of daylight and colour adaptation;

– To design, to assemble, and to adjust an experimental studies installation and to develop the software implementing the developed methodology;

– To evaluate the inaccuracy of the experimental and estimated results of the colour-matching functions of the physiological colorimetric system $(KZS)_{phys}$ $\overline{l}(\lambda)$, $\overline{m}(\lambda)$, $\overline{s}(\lambda)$ calculation obtained using the created installation.

2. METHOD OF DEFINITION OF THE SPECTRAL TRISTIMULUS VALUES

In [7–9], based on the statistical approach to detection and recognition of objects by VS, the major problems of creating the mathematical theory of threshold colour vision are formulated and partially solved. The threshold observation conditions are being considered because it is the first, the simplest level of the vision problem and its description allows us to reach good correspondence between the results of calculations based on statistical models and the results of experimental studies. It is important to note that the solutions are possible to be achieved with an arbitrary permanent decision-making algorithm even provided that the algorithm itself is unknown. Productivity of such approach is indicated by poor results of combination of statistical models with fixed signal processing algorithms such as 'maximum a posteriori probability (*MAP*)', 'minimum mean square error (*MMSE*)', etc. [10] with complex conditions over threshold where VS uses other, yet unknown algorithms.

For low-contrast images in the Weber-Fechner region, an expression was obtained which defines probability of detection P_{det} of an equally luminous colour object against a uniform colour background [8]:

$$P_{\text{det}} = \Phi(y), \tag{1}$$

where

$y = \dfrac{C_0 m_\Lambda - \dfrac{\ln \Lambda_{th}}{2}}{\sqrt{m_\Lambda}}$; $\Phi(y) = \dfrac{1}{\sqrt{2\pi}} \int\limits_{-\infty}^{y} \exp\left(-\dfrac{t^2}{2}\right) dt$ is the an integral of probability;

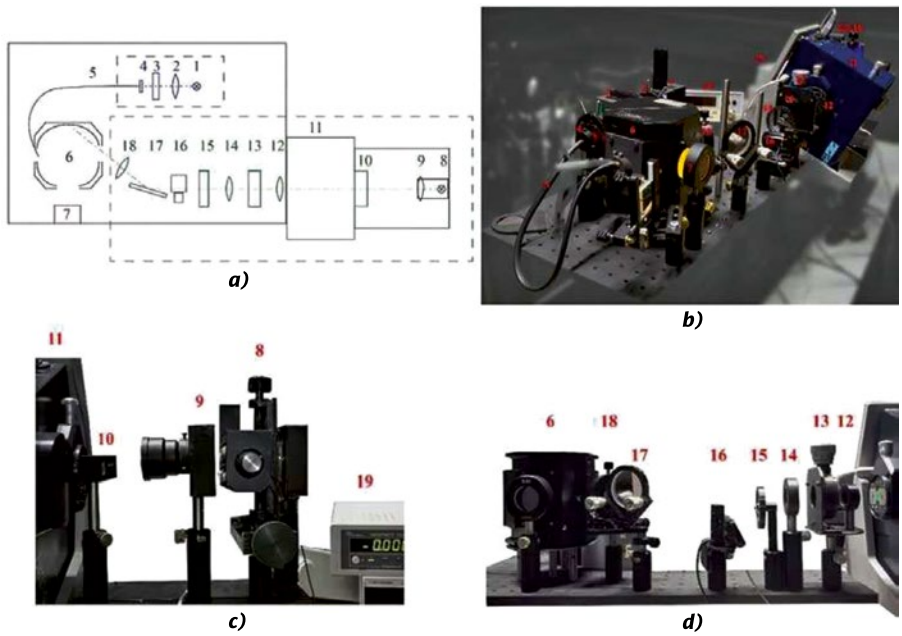

Fig. 2. The installation for the experimental studies: a – structural diagram; b – exterior of the main units; c – the illuminant of the object channel; d – the object forming and luminance adjusting unit

Λ_{th} is the threshold likelihood ratio defining the decision criterion in a statistic model of an optimal image detector [7]; in [9], the value $\ln(\Lambda_{th})=4.0$ was defined with confidence level of 0.95;

$$m_{\Lambda} = C_{1l}\left(\frac{\int_{380}^{780}\Delta L_{e\lambda o}(\lambda)\bar{l}(\lambda)d\lambda}{\int_{380}^{780}L_{e\lambda b}(\lambda)\bar{l}(\lambda)d\lambda}\right)^2 + C_{1m}\left(\frac{\int_{380}^{780}\Delta L_{e\lambda o}(\lambda)\bar{m}(\lambda)d\lambda}{\int_{380}^{780}L_{e\lambda b}(\lambda)\bar{m}(\lambda)d\lambda}\right)^2 + C_{1s}\left(\frac{\int_{380}^{780}\Delta L_{e\lambda o}(\lambda)\bar{s}(\lambda)d\lambda}{\int_{380}^{780}L_{e\lambda b}(\lambda)\bar{s}(\lambda)d\lambda}\right)^2;$$

where $\Delta L_{e\lambda o}(\lambda) = L_{e\lambda o}(\lambda) - L_{e\lambda b}(\lambda)$ is the difference between spectral distributions of radiance of an object and background; $L_{e\lambda o}(\lambda)$is spectral distribution of an object radiance; $L_{e\lambda b}(\lambda)$ is spectral distribution of background radiance; $\bar{l}(\lambda)$, $\bar{m}(\lambda)$, $\bar{s}(\lambda)$ are the colour-matching functions of the physiological colorimetric system;

C_0, C_{1l}, C_{1m}, C_{1s} are the constant factors of the statistical model which do not depend on λ and do not depend on luminance in the Weber-Fechner region. They depend on individual characteristics of VS (observer) and are defined when normalizing the statistical model.

$\bar{l}(\lambda)$, $\bar{m}(\lambda)$, $\bar{s}(\lambda)$ are the indefinite functions of the mathematical model and it appears impossible to obtain them on basis of expressions (1), since the same probability of detection may be obtained with different values of these functions. The problem simplifies significantly by considering threshold detection of monochromatic objects against any coloured (in particular, white) background. In this case, since the argument y in the expression (1) equals to zero, the following expression derives from it:

$$C_{1l}\left(\frac{L_{eo}^{th.dif}(\lambda)\bar{l}(\lambda)}{\int_{380}^{780}L_{e\lambda b}(\lambda)\bar{l}(\lambda)d\lambda}\right)^2 + C_{1m}\left(\frac{L_{eo}^{th.dif}(\lambda)\bar{m}(\lambda)}{\int_{380}^{780}L_{e\lambda b}(\lambda)\bar{m}(\lambda)d\lambda}\right)^2 + C_{1s}\left(\frac{L_{eo}^{th.dif}(\lambda)\bar{s}(\lambda)}{\int_{380}^{780}L_{e\lambda b}(\lambda)\bar{s}(\lambda)d\lambda}\right)^2 = \frac{\ln\Lambda_{th}}{2C_0}. \quad (2)$$

After introducing the indexes $C_1 = \sqrt{\frac{\ln\Lambda_{th}}{2C_0C_{1s}}}$, $C_2 = \frac{C_{1l}}{C_{1s}}$, $C_3 = \frac{C_{1m}}{C_{1s}}$, the expression of threshold difference between object and background radiances ($L_{eo}^{th\,dif}(\lambda)$) derives from (2):

$$L_{\text{eo}}^{th.dif}(\lambda)=$$

$$=\frac{C_1}{\sqrt{C_2\left(\frac{\overline{l}(\lambda)}{\int_{380}^{780}L_{\text{e}\lambda\text{b}}(\lambda)\overline{l}(\lambda)d\lambda}\right)^2+C_3\left(\frac{\overline{m}(\lambda)}{\int_{380}^{780}L_{\text{e}\lambda\text{b}}(\lambda)\overline{m}(\lambda)d\lambda}\right)^2+\left(\frac{\overline{s}(\lambda)}{\int_{380}^{780}L_{\text{e}\lambda\text{b}}(\lambda)\overline{s}(\lambda)d\lambda}\right)^2}}. \quad (3)$$

Conventional definition of $\overline{l}(\lambda)$, $\overline{m}(\lambda)$, $\overline{s}(\lambda)$ from (3), by solving the system of *n* equations, (4),

$$L_{\text{eo}}^{th.dif}(\lambda_1)=$$

$$=\frac{C_1}{\sqrt{C_2\left(\frac{\overline{l}(\lambda_1)}{\int_{380}^{780}L_{\text{e}\lambda\text{b}}(\lambda)\overline{l}(\lambda)d\lambda}\right)^2+C_3\left(\frac{\overline{m}(\lambda_1)}{\int_{380}^{780}L_{\text{e}\lambda\text{b}}(\lambda)\overline{m}(\lambda)d\lambda}\right)^2+\left(\frac{\overline{s}(\lambda_1)}{\int_{380}^{780}L_{\text{e}\lambda\text{b}}(\lambda)\overline{s}(\lambda)d\lambda}\right)^2}},$$

$$L_{\text{eo}}^{th.dif}(\lambda_2)=$$

$$=\frac{C_1}{\sqrt{C_2\left(\frac{\overline{l}(\lambda_2)}{\int_{380}^{780}L_{\text{e}\lambda\text{b}}(\lambda)\overline{l}(\lambda)d\lambda}\right)^2+C_3\left(\frac{\overline{m}(\lambda_2)}{\int_{380}^{780}L_{\text{e}\lambda\text{b}}(\lambda)\overline{m}(\lambda)d\lambda}\right)^2+\left(\frac{\overline{s}(\lambda_2)}{\int_{380}^{780}L_{\text{e}\lambda\text{b}}(\lambda)\overline{s}(\lambda)d\lambda}\right)^2}}$$

$$L_{\text{eo}}^{th.dif}(\lambda_n)=$$

$$=\frac{C_1}{\sqrt{C_2\left(\frac{\overline{l}(\lambda_n)}{\int_{380}^{780}L_{\text{e}\lambda\text{b}}(\lambda)\overline{l}(\lambda)d\lambda}\right)^2+C_3\left(\frac{\overline{m}(\lambda_n)}{\int_{380}^{780}L_{\text{e}\lambda\text{b}}(\lambda)\overline{m}(\lambda)d\lambda}\right)^2+\left(\frac{\overline{s}(\lambda_n)}{\int_{380}^{780}L_{\text{e}\lambda\text{b}}(\lambda)\overline{s}(\lambda)d\lambda}\right)^2}} \quad (4)$$

is impossible, since:

– To calculate $L_{\text{eo}}^{th.dif}(\lambda_1)$ using (3), three values are necessary: $\overline{l}(\lambda)$, $\overline{m}(\lambda)$, $\overline{s}(\lambda)$, i.e. the number of unknown variable in the system of equations (4) is always twice as many as the number of equations;

– To calculate the integrals which this system contains, it is necessary to know the required functions $\overline{l}(\lambda)$, $\overline{m}(\lambda)$, $\overline{s}(\lambda)$ within the entire visible spectre region, and they are unknown in the beginning of the calculation.

The solution was found by analysing possible forms of the functions $\overline{l}(\lambda)$, $\overline{m}(\lambda)$, $\overline{s}(\lambda)$. The analysis of the data presented in [11, 12] has shown that $\overline{m}(\lambda)$ is symmetric function with one maximum whereas $\overline{l}(\lambda)$ and $\overline{s}(\lambda)$ are asymmetrical functions with one maximum. Preliminary calculations have shown that the best results (at minimum values of the unknown factors) are obtained by means of approximation of $\overline{m}(\lambda)$ by a quadratic exponent with unknown positions of the maximum and value of half-width and approximation of $\overline{l}(\lambda)$ and $\overline{s}(\lambda)$ by a quadratic exponent with unknown maximums and half-widths different in the short-wave and long-wave parts of the spectre with respect to the maximums. The approximation error of these subjects with respect to all known dependences $\overline{l}(\lambda)$, $\overline{m}(\lambda)$, $\overline{s}(\lambda)$ [1, 6, 9, 11, 12] does not exceed 1 %, which is much less than the natural scatter of observer's characteristics of (15–25) %. Since, as noted previously [8], likelihood ratio does not depend on the maximum values of $\overline{l}(\lambda)$, $\overline{m}(\lambda)$, $\overline{s}(\lambda)$, the system of equations (4) will comprise eleven unknown

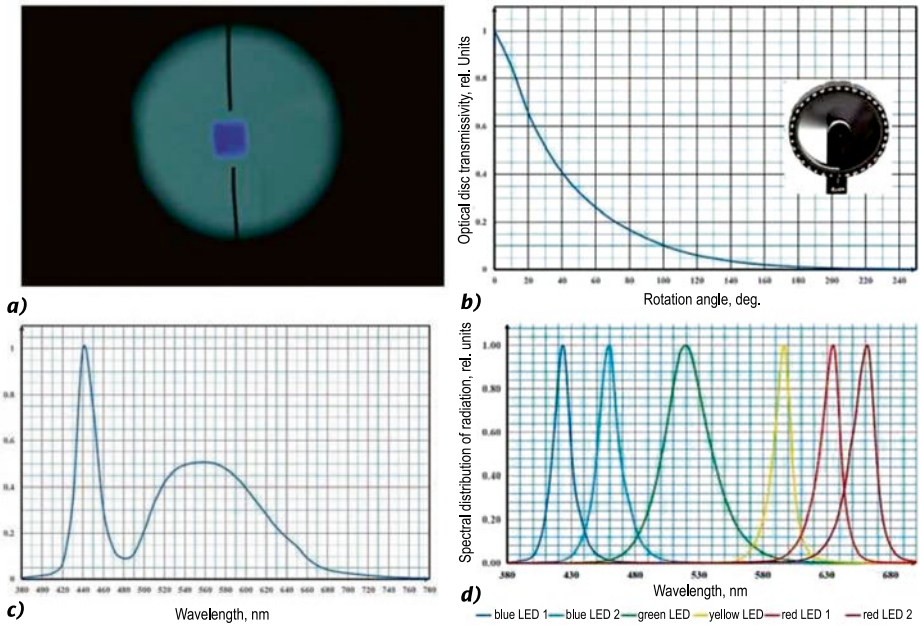

Fig. 3. Characteristics of the elements of the installation for the experimental studies: a – the view of the image through the ocular **7**; b – the dependence of the optical disc transmissivity on the rotation angle relative to the axis; c – the radiation spectrum of the white LED of the background channel; d – radiation spectra of the coloured LEDs of the object channel

variables (including C_1–C_3), which makes it possible to solve this system if the number of experimental values of $L_{eo}^{th.dif}(\lambda_1)$ is at least equal to 11. To implement this part of the developed method, the installation for determination of thresholds of detection of monochromatic objects $L_{eo}^{th.dif}(\lambda_1)$ against coloured (including white) backgrounds by a spectator was designed. Analysis of the methods of obtainment of the VS threshold characteristics [11, 12] has shown that the method of minimal changes is the least difficult, therefore, it was selected as the basis of the developed installation.

3. THE INSTALLATION FOR EXPERIMENTAL STUDIES

3.1. Description of the Installation

The installation is assembled on two optical flats using standard fasteners and transporters of optical parts by *Cobra Optics*, Special Systems, etc. The installation, Fig. 2, consists of the following components: the background radiation forming channel (*1–5*); the object image forming channel (*8–18*); the integrating sphere (*6*) combining radiation of these two channels and the ocular (*7*) for observing the object image on the wall of the integrating sphere (*6)*.

Radiation in the background channel is emitted by means of a white LED (*1*) by *Cree* with power of 5 W and correlated colour temperature T_{cp} of 4800 *K*. Its spectral response characteristics are shown in Fig. 3. The radiation of the LED is focused by the lens *YUCON NVMT* 50 mm (*2*) with relative aperture 1:1.4, passes through the filter unit (*3*) and is focused at the input end of the O-S illuminating fibre-optic bundle (*4*) with diameter of 5 mm manufactured by the LZOS factory. From its output end (*5*) radiation of the background channel is transferred to the *UKU120* photometer sphere (*6*) by *Opsira* (*CZL*) with a diameter of 120 mm.

The calculation has shown that the white LED in the object channel does not provide necessary radiant flow at borders of the visible range of the spectrum even at power of 20 W, therefore, 6 coloured LED's with power of 5 W by *Cree* were selected as sources of radiation. Their radiation spectra are shown in Fig. 3. The LEDs are placed in two rows on a vertical board with the displacement mechanism *8,* which allows setting of the LEDs on the optical axis of the lens *9* with relative aperture 1:1 and focus distance of 37 mm.

After passing the electro-mechanic shutter, the image of the LEDs emitting area *10* is built by the lens *9* at the entrance slit of the double monochromator *11 MSA-130* by *TOPAG Lasertechnik GmbH* with diffraction gratings of 600 slits per mm operating in the dispersion subtraction mode. By means of the condenser lens *12*, the monochromatic radiation illuminates the optical slit *13 SXM-1* by *SOLAR Laser Systems* forming the dimensions of the observed object (2° at output of the ocular (*7*)). The transfer optics *14* illuminates the optical wedge *15 OMMB-NDFC50* by Special Systems, Fig. 3, ad-

justing gradually luminance of the object. The lighter and the video camera *16* provide reading of the scale of the optical wedge. The lens *18* and the rotary mirror *17* build the image of the object on the wall of the photometry sphere *6*. The form of the image observed through the ocular *7* is shown in Fig. 3. The vertical orienting markers and the shutter *10* reduce dispersion of the observer's answers related to search for the object in the field of view and in the course of its observation, which reduces the measurement error.

3.2. Calibration of the Installation

In order to reduce the error of the installation, relative measurements of all spectral characteristics of its elements were conducted at output of the installation (behind the ocular (**7**)) by means of the monochromator LOMO MDR-206 with 1200 silts per mm diffraction grating and the detector unit with a silicon photodiode for the range of (200–1100) nm (with error of ±0.5 nm). The measured spectral characteristics of the elements of the installation are presented in Fig. 3. Absolute calibration of the installation was conducted by means of a *PIN* photodiode *SD444–12–12–171* calibrated by VNIIOFI based on absolute current responsivity within the range of (300–1100) nm. Stabilised power supply units *QJ3005C* were used for power supply of the LEDs of the installation and the modes of their power supply were controlled by digital ammeter *CA3010/3–000* (*19*) with measurement accuracy of 0.1. For monitoring of luminance at output of the ocular (*7*), the *Konica Minolta LS-110* luminance meter was used.

Based on calculations and multiple measurements (more than 20 repetitive measurements of spectral and light characteristics), it was found that repeatability error of $L_{co}(\lambda)$ and $L_{cb}(\lambda)$ as well as of background luminance at output of the ocular *7* of the installation does not exceed 7 %.

3.3. Software and Calculation Inaccuracy

To implement the second part of the method of $\overline{l}(\lambda)$, $\overline{m}(\lambda)$, $\overline{s}(\lambda)$ definition by solving the system of equations (4), a software was designed for solving of this system using the least squares method [13]. Given that the left-hand side of (4) is defined with inevitable error, it was required to define acceptable measurement error of $L_{co}^{th.dif}(\lambda_1)$ in the system (4) and acceptable deviations of the initial assessments of $\overline{l}(\lambda)$, $\overline{m}(\lambda)$, $\overline{s}(\lambda)$ from their true values providing convergence of the true values of $\overline{l}(\lambda)$, $\overline{m}(\lambda)$,$\overline{s}(\lambda)$ obtained by means of the least squares method. The values obtained in [9] and approximated by the following functions were used as the test of $\overline{l}(\lambda)$, $\overline{m}(\lambda)$, $\overline{s}(\lambda)$ values:

$$\overline{l}(\lambda)=\frac{f_l(\lambda)}{2}\exp\left\{-\left[\frac{(\lambda-\lambda_{lm})}{\sigma_l}\right]^2\right\}+$$
$$+\frac{1-f_l(\lambda)}{2}\exp\left\{-\left[\frac{(\lambda-\lambda_{lm})}{C_l\sigma_l}\right]^2\right\},$$
$$\overline{m}(\lambda)=\exp\left\{-\left[\frac{(\lambda-\lambda_{mm})}{\sigma_m}\right]^2\right\},$$
$$\overline{s}(\lambda)=\frac{f_s(\lambda)}{2}\exp\left\{-\left[\frac{(\lambda-\lambda_{sm})}{\sigma_s}\right]^2\right\}+$$
$$+\frac{1-f_s(\lambda)}{2}\exp\left\{-\left[\frac{(\lambda-\lambda_{sm})}{C_s\sigma_s}\right]^2\right\}, \quad (5)$$

where λ_{lm}, λ_{mm}, λ_{sm} are wavelengths at which the functions reach their maximums; σ_l, σ_m, σ_s are the parameters defining half-width of the functions; $f_l(\lambda)$ and $f_s(\lambda)$ are functions equal to one if $\lambda<\lambda_{lm}$ and $\lambda<\lambda_{sm}$ respectively or to zero in the opposite cases.

The effect of the calculation error of $L_{co}^{th.dif}(\lambda_1)$ on the calculation error of the parameters λ_{lm}, λ_{mm}, λ_{sm} and σ_l, σ_m, σ_s at random scatter of the test evaluations $\overline{l}(\lambda)$, $\overline{m}(\lambda)$, $\overline{s}(\lambda)$ was studied. The scatter of values of $L_{co}^{th.dif}(\lambda_1)$ and initial evaluations of λ_{lm}, λ_{mm}, λ_{sm} and σ_l, σ_m, σ_s corresponded to the normal law of distribution with different standard deviations (SD) with respect to their test values. Then the system of equations (4) was solved and the calculated (p) of the function of $\overline{l}(\lambda)$, $\overline{m}(\lambda)$, $\overline{s}(\lambda)$, were defined using the expressions (5), then the errors in deviation of λ_{lm}, λ_{mm}, λ_{sm} and σ_l, σ_m, σ_s with respect to their test values were calculated as well as the integral curve difference criterion defined (for $\overline{l}(\lambda)$) as:

$$f_{\text{int}}^{l}(\sigma_L)=\frac{\int_{380}^{780}\left|\overline{l}(\lambda)-\overline{l}_{\hat{n}}(\lambda)\right|d\lambda}{\int_{380}^{780}\overline{l}(\lambda)d\lambda}, \quad (6)$$

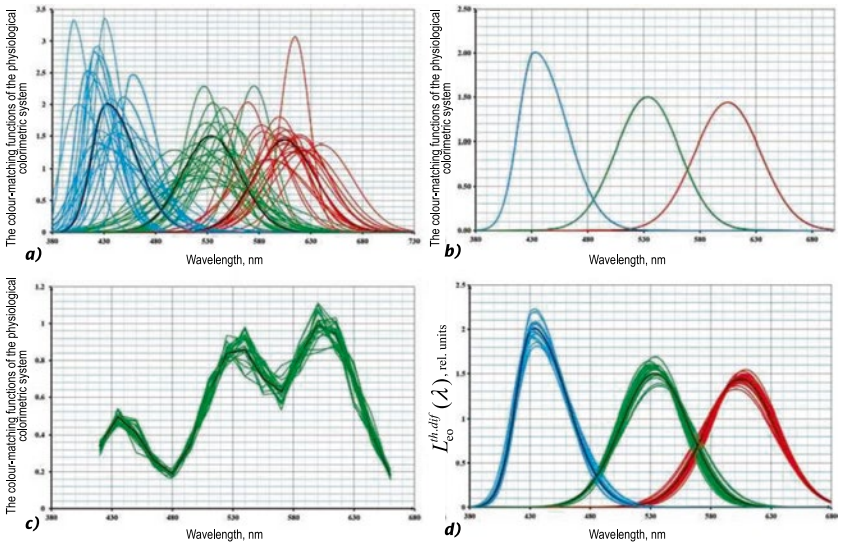

Fig. 4. The results of calculation with scatter of λ_{lm}, λ_{mm}, λ_{sm} equal to 11 nm and scatter of λ_{lm}, λ_{mm}, λ_{sm} equal to 16 nm at σ_L = = 0 (a, b) and 7.5 % (c, d), the test graphs are shown in black

where $\overline{l}_{\tilde{n}}(\lambda)$ and $\overline{l}(\lambda)$ are the calculated and the test functions $\overline{l}(\lambda)$; $\sigma_L = \dfrac{\overline{\sigma}_L}{L_{eo}^{th.dif}(\lambda)}$ is relative SD of scatter of the test values of $L_{eo}^{th.dif}(\lambda)$.

The functions $f_{int}^{m}(\sigma_L)$ and $f_{int}^{s}(\sigma_L)$ for $\overline{m}(\lambda)$ and $\overline{s}(\lambda)$ are calculated in a similar way.

Fig. 4, (*a*) presents 20 initial evaluations of $\overline{l}(\lambda)$, $\overline{m}(\lambda)$, $\overline{s}(\lambda)$, with scatter of σ_l, σ_m, σ_s equal to 30 % (average 11 nm) and scatter of λ_{lm}, λ_{mm}, λ_{sm} equal to 3 % (average 16 nm), and Fig. 4, (*b*) presents the graphs of the functions of $\overline{l}(\lambda)$, $\overline{m}(\lambda)$, $\overline{s}(\lambda)$, obtained using the equations (4) with $\sigma_L = 0$.

Since all the 20 solutions are the same, convergence of the least squares method in this case is at least 95 %. If an error appears in the input values of $L_{eo}^{th.dif}(\lambda_1)$, the functions $\overline{l}_c(\lambda)$, $\overline{m}_c(\lambda)$, $\overline{s}_c(\lambda)$ are defined inaccurately. Fig. 4, (*c*) presents 20 graphs of $L_{eo}^{th.dif}(\lambda_1)$ obtained for σ_L =7.5 % and Fig. 4, (*d*) presents 20 graphs of $\overline{l}_c(\lambda)$, $\overline{m}_c(\lambda)$, $\overline{s}_c(\lambda)$ corresponding to these $L_{eo}^{th.dif}(\lambda_1)$. Fig. 5, (*a*) presents the graphs of the integration functions of (6).

The dependences of the errors of definition of the parameters λ_{lm}, λ_{mm}, λ_{sm} и σ_l, σ_m, σ_s as well as the integral criteria $f_{int}^{l}(\sigma_L)$, $f_{int}^{m}(\sigma_L)$, $f_{int}^{s}(\sigma_L)$ on SD of scatter of the parameters of initial evaluations and σ_L were studied. The results of the corresponding calculations are presented in Fig. 5, (*b–d*). They have demonstrated that the errors of definition of the parameters λ_{lm}, λ_{mm}, λ_{sm} и σ_l, σ_m, σ_s are monotonously related to the integral criteria $f_{int}^{l}(\sigma_L)$, $f_{int}^{m}(\sigma_L)$, $f_{int}^{s}(\sigma_L)$ and, therefore, only the graphs of the integral error criteria are presented.

4. DISCUSSION OF THE RESULTS

4.1. Preliminary Results

The measurement error of $L_{eo}^{th.dif}(\lambda_1)$ affects the definition error of $\overline{l}(\lambda)$, $\overline{m}(\lambda)$, $\overline{s}(\lambda)$, in the most significant way. This error affects definition of $\overline{l}(\lambda)$ the least. For $\overline{m}(\lambda)$ and $\overline{s}(\lambda)$, with $L_{eo}^{th.dif}(\lambda_1)$ definition error of 12 %, the values of $f_{int}^{m}(\sigma_L)$ and $f_{int}^{s}(\sigma_L)$ exceed 7.5 %.

Inaccuracy in setting the initial evaluations σ_l, σ_m, σ_s equal to even 40 % (about 15 nm) and that of λ_{lm}, λ_{mm}, λ_{sm} equal to 4 % (about 21 nm) does not lead to reduction of convergence of the least squares method and inaccuracy of definition of $\overline{l}(\lambda)$, $\overline{m}(\lambda)$, $\overline{s}(\lambda)$. The values of all integral error criteria do not exceed the round-off error in this case.

To check the applicability of the created method and the installation, a test experiment involving three trained observers was conducted and it demonstrated high sensitivity of the method allowing us to define individual distinctions of their colour-matching functions. Average values of the approximation parameters as per the expressions (5) for these three observers are as follows: λ_{lm} = 601.3 nm, σ_l = 45.25 nm, C_l =1.037; λ_{mm} = 542.2 nm, σ_m = 41.2 nm; λ_{sm} = 441.9 nm, σ_s = 25.2 nm, C_s = 1.19. Of course, these results are just preliminary and a larger number of spectators shall be tested using the developed method to draw final conclusions. This will allow us to understand whether it is possible to align the achieved results with the international system *XYZ*.

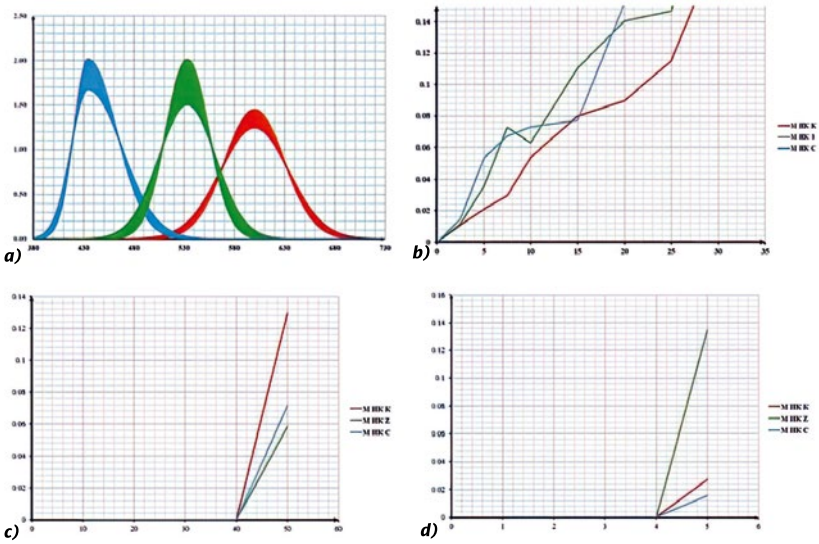

Fig. 5. The integral functions of the integral criterion with definition error of σ_l, σ_m, σ_s (*a*); the dependence of the integral approximation error $f_{\text{int}}^{l}(\sigma_L)$ (*integral criterion L*), $f_{\text{int}}^{m}(\sigma_L)$ (*integral criterion M*) and $f_{\text{int}}^{s}(\sigma_L)$ (*integral criterion S*) on σ_{L} (*b*); SD of the scatter of the initial evaluations of σ_l, σ_m, σ_s (*c*); SD of the scatter of the initial evaluations of λ_{lm}, λ_{mm}, λ_{sm} (*d*)

4.2. Discussion

Many researchers measured of tristimulus values in conditions over threshold [12], but the experimental methods and installations for measurements of colour threshold are described only in the works by MacAdam and Brown [14, 15]. It turned out that in the case of the method with changes in chromaticity coordinates (without changing adaptation luminance) below the threshold value used in their experiments, large scatter of the results for different observers appeared, which did not allow defining any patterns for a set of observers. This was primarily explained by complexity of the method since 5 values should be set and adjusted to obtain one experimental value: background luminance, luminance of three reference chromaticity channels and luminance of the channel of the studied monochromatic source of radiation. As a result, acceptable values were obtained only for one spectator (*Perley G. Nutting*), they are presented in [14]. Further experiments with changing background luminance [15] and other studies also did not allow identifying any general dependence.

The method suggested in this work is based on object detection experiments, which provides significantly less variation and scatter of results as compared to the method of equalisation of chromaticity or colours. Moreover, the developed method requires only two measurements in each experimental point (object and background luminance) instead of five as in the case of the chromaticity equalisation method, which reduces the error of the results.

5. CONCLUSIONS

1. Based on the statistical theory of threshold colour vision, the method of definition of spectral sensitivities of the L-cones, M-cones and S-cones of human vision system (VS) in conditions of natural colour adaptation was developed.

2. The designed and assembled installation for studying of VS threshold characteristics allows us to maintain output parameters of the observed images in the course of the experiments with error not exceeding 7 %.

3. The software was developed for solving of the system of nonlinear equations of the statistical model of threshold colour vision by means of the least squares method, the study of which has demonstrated convergence of the method with significant (about 15 nm) deviation of the initial evaluations of the required parameters from their true values.

4. According to the materials presented in [11], natural scatter of VS characteristics for a set of observers is equal to (15–25)%. If we set the summarised error of definition of $\overline{l}(\lambda)$, $\overline{m}(\lambda)$, $\overline{s}(\lambda)$ equal to 10 %, we can see that the value of σ_{L} obtained experimentally by means of the installation should not exceed 7 %. This result may be obtained by increasing the number of multiple measurements of $L_{\text{eo}}^{th.dif}(\lambda_i)$ since this component of the error decreases in inverse proportion to the square root of this number [13].

5. When solving the system of equations (4) by means of the least squares method, the results of calculations shall be checked. If the obtained values of parameters σ_l, σ_m, σ_s are different from their

initial evaluations by more than 15 nm and those of λ_{lm}, λ_{mm}, λ_{sm} are different from the initial evaluations by more than 21 nm, it is necessary to conduct another calculations with new initial evaluations.

REFERENCES

1. Yustova E.N. Definition of Coordinate Axes of the Main Physiological System Based on Tests Involving Colour-Blinds [Opredeleniye koordinatnykh osey osnovnoy fiziologicheskoy sistemy iz opytov s tsvetnoslepymi] // Proceedings of the Academy of Sciences of the USSR, 1948, Vol. 63, # 4, pp. 383–385.

2. CIE170–1:2006 Fundamental Chromaticity Diagram with Physiological Axes – Part 1.

3. Stockman A., Lindsay T., Sharpe B. The spectral sensitivities of the middle- and long-wavelength-sensitive cones derived from measurements in observers of known genotype // Vision Research, 2000, Vol. 40, pp. 1711–1737.

4. Stockman A., MacLeod D.I.A., Vivien J.A. Isolation of the middle- and long-wavelength sensitive cones in normal trichromats // J. Opt. Soc. Am. A.,1993, Vol. 10, pp. 2471–2490.

5. König A., Dieterici C. Die Grundempfindungen und ihre Inlensitäts-Vertheilung im Spectrum// Siz. Akad. Wiss. Berlin, 1886, pp. 805–829.

6. Stockman A. Cone fundamentals and CIE standards // Current Opinion in Behavioral Sciences, 2019, Vol. 30, pp. 87–93.

7. Boos George V. The Probability of Detecting Coloured Objects on Coloured Backgrounds Based on a Statistical Model of the Threshold of Colour Vision // Light & Engineering Journal, 2018, Vol. 26, # 2, pp. 14–19.

8. Boos George V. and Grigoryev Andrey A. New Approach in the Determination of Qualitative Characteristics of Outdoor Illumination// Light & Engineering Joural, 2016, Vol. 24, # 1, pp. 51–57.

9. Grigoriev, A.A., Gordyukhina, S.S. The Method of Definition of Sensitivity of RGB Receptors Based on the Statistical Model of a Vision Organ [Metod opredeleniya chuvstvitelnosti K, Z, S-retseptorov na osnove statisticheskoy modeli organa zreniya] // Bulletin of MEI, 2010, Vol. 2, pp. 174–178.

10. Brainard D.H., Freeman W.T. Bayesian color constancy // J. Opt. Soc. Am. A., 1997, Vol. 14, #7, pp. 1393–1411.

11. Judd D., Wyszecki G. Color in Business, Science, and Industry, Moscow: Mir, 1978, 592 p.

12. Meshkov V.V., Matveev A.B. Basics of Light Engineering: Study Guide for Higher Education Institutions: in 2 parts. P. 2. Physiological Optics and Colorimetry [Osnovy svetotekhniki: uchebnoye posobiye dlya vuzov: v 2 ch. Ch. 2. Fiziologicheskaya optika i kolorimetriya, 2nd Edition, revised and supplemented, Moscow: Energoatomizdat, 1989, 432 p.

13. Linnik Yu.V. The Least Squares Method and Basics of Mathematical and Statistical Theory of Observations Processing [Metod naimenshikh kvadratov i osnovy matematiko-statisticheskoy teorii obrabotki nablyudeniy], 2nd edition, Moscow: Gos. Izd-vo Phyz.-Math. Lit, 1962, 354 p.

14. MacAdam D.L. Visual Sensitivities to Color Differences in Dayling // J. Opt. Soc. Am., 1942, Vol. 32, pp. 247–274.

15. Brown W.R.L., MacAdam D.L. Visual sensitivities to combined chromaticity and luminance differences // J. Opt. Soc. Am., 1949, Vol. 39, # 10, pp. 808–834.

George V. Boos**,**
Ph. D. In 1986, he graduated from the Moscow Power Engineering Institute (MEI). At present, he is the President of MSK BL GROUP, Head of the Light and Engineering sub-department of NIU MEI. He is Recipient of the State Prize of the Russian Federation for Architectural Lighting of Moscow, the Chairman of the Science and Engineering board Svetotekhnika and of the editorial board of the Svetotekhnika/Light & Engineering journal

Andrey A. Grigoryev,
Doctor of Technical Sciences, Professor. In 1981, he graduated from the Moscow Power Engineering Institute (MEI). At present, he is the Professor of the Lighting Engineering sub-department of NIU MEI, the Head of the Vision Functions Research Group at Sergey Vavilov Russian Lighting Research Institute (VNISI)

Viktoria A. Rybina*,*
engineer. In 2018, she graduated from NIU MEI. At present, she is postgraduate student and teaching assistant of the Light and Engineering sub-department of NIU MEI, junior researcher of the Vision Functions Research Group of Sergey Vavilov Russian Lighting Research Institute (VNISI)